Theoretical and Applied Fracture Mechanics 130 (2024) 104273

Contents lists available at ScienceDirect

Theoretical and Applied Fracture Mechanics

journal homepage: www.elsevier.com/locate/tafmec

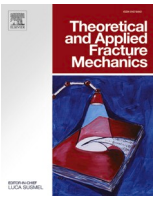

Fracture prediction in flat PMMA notched specimens under tension - effectiveness of the equivalent material concept and fictitious material concept

Elżbieta Bura [a,*], A.R. Torabi [b], Andrzej Seweryn [c]

[a] Faculty of Mechanical Engineering, Bialystok University of Technology, Poland
[b] Department of Mechanical Engineering, Auburn University, Auburn, AL 36849, USA
[c] Faculty of Mechanical Engineering and Ship Technology, Gdansk University of Technology, Poland

ARTICLE INFO

Keywords:
PMMA
Fracture
rounded V-notch
equivalent material concept (EMC)
fictitious material concept (FMC)

ABSTRACT

The fracture of notched elements under mode I loading (tension) remains an inexhaustible research topic, especially when it comes to the fracture of thermoplastic materials such as polymethylmethacrylate (PMMA), which experience considerable plastic strains under tension. The paper points out that traditional brittle fracture criteria such as mean stress (MS) or maximum tangential stress (MTS) criteria used to predict this phenomenon do not accurately indicate the value of the critical load. They work much better when combined with the equivalent material concept (EMC) and fictitious material concept (FMC). The effectiveness of both concepts depends on the size of the notch root radius, and thus on the yield zone size.

1. Introduction

Structural elements weakened by notches, i.e. holes or slots, are particularly prone to failure through cracking. The crack initiation moment is influenced not only by the element geometry, but also by the load type or the material from which the element is made. External factors such as temperature also determine the course of the fracture process. All this shows the complexity of this phenomenon, which is why it is the research subject of many experimental and theoretical works, the main goal of which is to formulate effective tools for predicting the moment and location of crack initiation, as well as the direction of its propagation.

It seems that the most well-studied type of fracture is the brittle fracture of notched elements observed during the first type of notch/gap deformation, i.e. tension or bending (depending on the type of specimen used). Many research papers have described this phenomenon in terms of experimental, numerical and theoretical studies. A material very often studied in the context of brittle fracture is polymethylmethacrylate (PMMA). It is a thermoplastic with a wide range of applications in many industries. Today, special interest in this material is due to its biocompatibility, allowing PMMA to be used in medicine. The results of experimental tension tests of flat V-notched specimens have been described in the work of Seweryn [1], which analysed the effect of notch opening angle on the value of failure load. A fracture criterion based on the values of the stress intensity factors and the Novozhilov [2] criterion was proposed. In the work of Ayatollahi et al. [3], the first type of the notch deformation was analysed experimentally and theoretically for five different samples. Despite the same loading method, the crack propagation trajectories were found to be significantly different. The effectiveness of predicting the crack propagation path was verified using the strain energy density criterion [4]. Aliha et al. [5] tested beam specimens made of PMMA under three-point bending, so that fracture was observed during the I, II, and mixed I + II types of notch deformation. Different loading speeds were taken into account, and the theoretical considerations compared the effectiveness of the fracture prediction using criteria such as maximum tangential stress (MTS) and generalised maximum tangential stress (GMTS). The fracture of PMMA at different loading speeds has also been described in the work of Bura and Seweryn [6], Acharya and Mukhopadhyay [7] or, for example Wada et al. [8]. Elements made of PMMA and weakened with U-notches were tested under simple and complex loading conditions, which were realised by changing the angular position of the notch axis with respect to the axis of the acting tensile load [9]. The effectiveness of fracture prediction using the average strain energy density (ASED) [10] criterion was tested, which states that the crack initiates when the average value of the strain energy density measured over a control volume is equal to a critical value. A similar type of PMMA element was used in the

* Corresponding author.
E-mail addresses: e.bura@pb.edu.pl (E. Bura), a_torabi@auburn.edu (A.R. Torabi), andrzej.seweryn@pg.edu.pl (A. Seweryn).

https://doi.org/10.1016/j.tafmec.2024.104273
Received 7 November 2023; Received in revised form 3 January 2024; Accepted 6 January 2024
Available online 13 January 2024

Nomenclature

ASED	average strain energy density
SED	strain energy density
GMTS	generalised maximum tangential stress
EMC	equivalent material concept
FMC	fictitious material concept
MTS	maximum tangential stress
MS	mean stress
TCD	theory of critical distances
A_{real}	actual cross-sectional area of specimen
A_0	initial cross-sectional area of specimen
E	Young's modulus
E^{FMC}	Young's modulus for virtual material (FMC)
F	tensile force
K_{IC}	critical stress intensity factor
Δl	extension of the specimen measurement base
l_0	the initial specimen measurement base length
P_c^{exp}	average maximum force
r_c, d_c	critical distance
R_m (σ_u)	tensile strength
$R_{0.2}$	yield stress
t	specimen thickness
ε_{true}	true strain
ε_{eng}	engineering strain
ε_u	ultimate strain for virtual material (FMC)
σ_{true}	true stress
σ_{eng}	engineering stress
$\sigma_{\theta\theta}$	tangential stress
σ_c	critical stress
σ_f^*	tensile strength for the virtual material (EMC)
σ_f^{FMC}	tensile strength for the virtual material (FMC)
ρ	notch root radius
ν	Poisson's ratio

experimental studies described in the work of Zhong et al. [11] Based on the results, a formula for predicting the crack initiation angle at mixed-mode I + II loading was obtained. More experimental results and theoretical considerations on the fracture of PMMA parts under mode I loading can be found in the literature [12–17]. Fracture tests apply not only to pure PMMA, but very often to PMMA-based composites with applications in medicine or dentistry. The mechanical and extrusion properties of the PMMA-based composite depending on the proportion of filler have been compared in many studies available in the literature [18,19].

Most of the works have used the results of PMMA tests conducted at fairly high strain rates on thin parts, weakened by sharp notches or with small root radii. All these factors contribute to the fact that the obtained characteristics of this material are linear or close to linear elastic, and this makes it possible to ignore the occurrence of plastic strain in theoretical considerations and consider the fracture process as brittle. In view of this, effective prediction of this phenomenon, and thus prevention of its negative effects, was possible using classical brittle fracture criteria such as the strain energy density (SED) criterion, MTS criterion or mean stress (MS) criterion. The PMMA in many cases exhibits greater or lesser ductility depending on the loading conditions. In the presence of large notch rounding radii, when applying low strain rates or under elevated temperature conditions, a non-linear relationship between the load value and displacement of PMMA parts is noted. In such situations, the use of brittle fracture criteria to predict this process generates large errors. A solution to this problem has been proposed by Torabi in his works. The equivalent material concept (EMC) was first discussed in Torabi work [20]. The MS criterion, supplemented by the EMC, allowed a high degree of consistency between theoretical and experimental critical load values for notched elements made of steel. In subsequent works, Torabi successfully extended this concept to other load cases, specimen types and other materials [21,22], including PMMA [23,24].

However, this concept discussed above does not work in all cases, so Torabi and Kamyab [25] proposed the new fictitious material concept (FMC), which was originally used to predict the failure load values of steel (AISI 304) notched components subjected to tension. MS and MTS criteria were used in combination with FMC, which made it possible to successfully predict the experimental results. The concept discussed was successfully applied to predict the crack initiation moment of other metallic materials [26–29]. In the paper [30], the FMC was used in combination with the ASED criterion. The combined concept was applied to the case of fracture of SENB type specimens subjected to bending and made of glass fibre reinforced polyamide 6. Better results were obtained than for ASED-EMC. The approach to fracture prediction using classical brittle fracture criteria, in combination with EMC or FMC, facilitates low-complexity numerical calculations, and thus the desired result may be obtained faster. The proposed concepts are alternatives to criteria designed for typically ductile materials.

The present study analysed the results of experimental fracture of flat PMMA specimens made in two thickness variants and weakened with notches of different bottom rounding radii [31]. The aim of the study was to determine what efficiency of fracture prediction during type mode I, the MS and MTS brittle fracture criteria have, and to combine them with EMC and FMC. The paper points out that EMC was initially expected to be effective for PMMA, with many works confirming its effectiveness. Based on the results obtained, it was pointed out that this concept was ineffective for large notch radii, and the FMC-based approach worked better in these cases. It was emphasised that the use of EMC and FMC depends not only on the characteristics of the material, but also on the geometry of the notch, especially the notch root radius. This is mainly due to the influence of local plastic zones that form around the notch prior to the fracture instance.

2. Material and samples – Experimental data

In the present study, the results of fracture testing of flat notched parts previously published by Bura and Seweryn [31] were used. The specimens were made of polymethylmethacrylate (PMMA), the basic properties of which were determined in a static tensile test, are summarised in Table 1. The material used in the study was obtained in the form of cast panels commonly used. The cast plates were chosen because of the wide range of possible thicknesses; the influence of which on the course of the fracture process was studied in the experimental research. Regular PMMA was used in the experiment due to its high availability compared to oriented PMMA. The oriented PMMA is a regular PMMA heated above the glass transition temperature, then stretched in a certain direction and finally cooled. Such a process used for this material

Table 1
PLEXIGLAS®GS properties [31].

Property	Value	Unit
Young's modulus, E	3 254	MPa
Tensile strength, R_m	72.10	MPa
Yield stress, $R_{0.2}$	47.17	MPa
Poisson's ratio, ν	0.38	–
Critical stress intensity factor, K_{IC}	1.07	$MPa\sqrt{m}$

is aimed at obtaining anisotropic physical and mechanical properties. This type of material has been studied, for example by Du et al. [32] and Yan and Sun [33]. However, in this manuscript, it was decided to pay the main attention to investigating the properties of PMMA used most often in engineering operations, i.e. regular PMMA, which has isotropic properties.

The loading conditions adopted in the text make it possible to conclude that, at a given base displacement velocity, the tested PMMA is characterized by considerable strains under tension. Compared to the results presented in the paper by Zheng et al. [34] where the strain of PMMA at room temperature at rupture was about 2.5 %, the strain obtained in the manuscript in question of about 6 % (Fig. 1) was considered a considerable tensile strain.

Five unnotched specimens of each thickness were used to determine the value of the presented properties. The critical value of the stress intensity factor (K_{IC}) was determined in the three-point bending test of the PMMA specimen weakened by the pre-crack, carried out in accordance with ASTM D5045-14. The K_{IC} value was averaged on the basis of three tests. The value obtained is similar to those described in the papers by Qiu et al. [35] and Wiangkham et al. [36]. Fig. 1 shows the engineering and true tensile stress–strain curves of the smooth specimen, characterised by a rather strong nonlinearity (end of the curves correspond to the ultimate point). The engineering tensile curve was determined using the initial cross-sectional area of the sample at its measurement base. The true stress–strain curve was determined using the actual cross-sectional area of the sample at the measurement base. The change in cross-sectional dimensions over time was monitored using the ARAMIS 3D 4 M vision system, which allows non-contact measurement of the displacement of the test piece, so it was possible to track the displacement of the observed area in three different directions over time. The experimental studies and the parameters adopted are described in more detail in the paper by Bura and Seweryn [31].

Target fracture tests of notched specimens (shown in Fig. 2) were carried out on an MTS 809.10 testing machine, under displacement control, which was measured using an axial extensometer. Displacement was set at a speed of 2.4 mm/min (0.04 mm/s) on a base equal to 50 mm. A total of 18 specimens (3 samples of each type) were tested. The samples were weakened with notches of different bottom rounding radii: 0.5, 2 and 10 mm. The level of stress concentration does not change significantly by changing the notch tip radius from 4 mm to greater values, e.g., 10 mm, for which the production process is considerably simpler. Hence, any values of the notch tip radius greater than 4 mm can be arbitrarily selected for the fracture investigation, for which the results are intended to be compared with the results of the specimens with large stress concentrations (0.5 and 2 mm tip radii). As a result of the tests, the values of the measuring base maximum elongation and the maximum tensile force value at which crack initiation occurred were determined (Table 2).

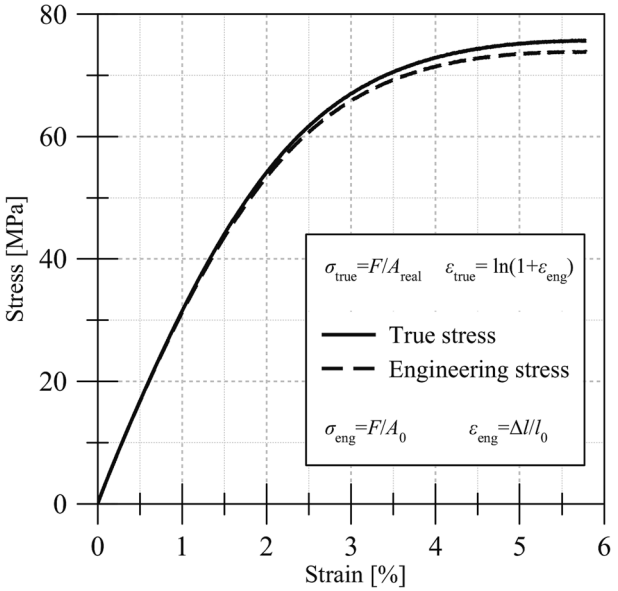

Fig. 1. Tensile stress–strain curves of PLEXIGLAS®GS [31].

3. Fracture criteria

To predict the fracture of PMMA notched specimens, brittle fracture criteria such as MS and MTS are the most commonly used. MTS criterion [37] assumes that brittle fracture initiates when the tangential stress $\sigma_{\theta\theta}$ at some critical distance r_c from the crack tip or notch bottom reaches a critical value equal to the material's tensile strength (σ_u) [38]:

$$\sigma_{\theta\theta}(r_c,\theta)=(\sigma_{\theta\theta})_c=\sigma_u \tag{3.1}$$

The distance r_c (see Fig. 3) for brittle materials takes the form [39–41]:

$$r_c=\frac{1}{2\pi}\left(\frac{K_{Ic}}{\sigma_u}\right)^2. \tag{3.2}$$

Equally often used with great success is the MS criterion [1,2], which assumes that the crack initiation from a notch or the propagation of a pre-existing crack occurs when the normal stress σ_n averaged over a certain distance d_c from the notch/crack reaches a critical value:

$$\overline{\sigma_n}=\frac{1}{d_c}\int_0^{d_c}\sigma_n dr=\sigma_u. \tag{3.3}$$

The use of the criterion forces the determination of two parameters. The critical stress value is usually equal to the tensile strength of the material R_m (σ_u) determined for a smooth specimen. The critical distance d_c (see Fig. 3) is additionally dependent on the material's fracture toughness K_{Ic} [1]:

$$d_c=\frac{2}{\pi}\left(\frac{K_{Ic}}{\sigma_u}\right)^2. \tag{3.4}$$

The values of the parameters necessary for using both above criteria have been established based on Eqs. (3.3) – (3.4) and K_{IC} (see Table 1).

For PMMA, which is generally considered a brittle material, high plasticisation and a non-linear stress–strain relationship are often observed. In such cases, classic brittle fracture criteria generate significant errors in predicting the critical load value. For improving the efficiency of predicting the crack initiation moment using MTS or MS criteria, the concepts proposed in Torabi's work can be employed.

The most popular concept is the equivalent material concept (EMC) applied along with brittle fracture criteria to ductile materials that exhibit relatively small deformation at failure. It is assumed that the SED (strain energy density) accumulated by the deformation process until necking of a real ductile material is equal to the SED of a typically brittle virtual material. At the same time, values of the Young's modulus for both materials are equal. In order to use this concept in conjunction with the MTS and MS criteria, the values of the following parameters were determined. Firstly, the tensile strength of the virtual material σ_f^*. The engineering tensile curve (Fig. 1) indicated the value of the strain ε_u corresponding to the tensile strength of the material (R_m, σ_c). Then, the true stress–strain curve was determined (Fig. 1). The SED was calculated using the area under the true stress–strain curve bounded by the previously determined strain value (Fig. 4):

$$\boldsymbol{SED}=\frac{\left(\sigma_f^*\right)^2}{2E}\rightarrow\sigma_f^* \tag{3.5}$$

The values of critical distances were determined based on Eqs. (3.3) – (3.4), where $\sigma_c=\sigma_f^*$ and K_{IC} is taken from Table 1.

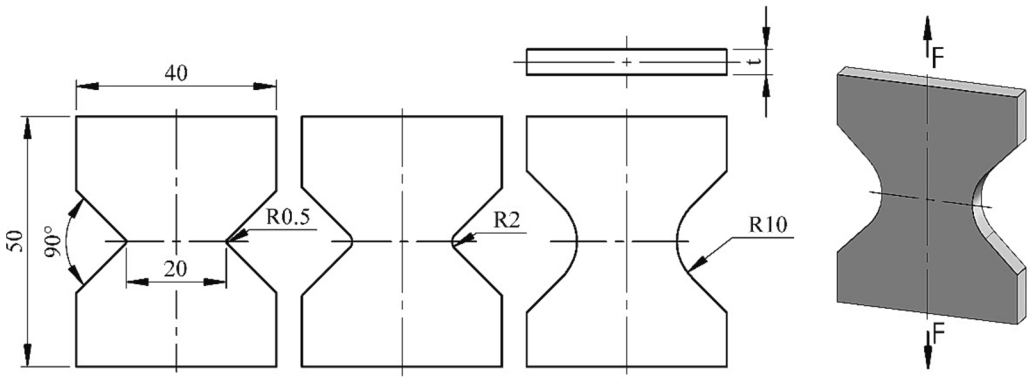

Fig. 2. Notched specimens [31].

Table 2
Critical tensile force values for notched specimens subjected to uniaxial tension [31].

Notch root radius	Average specimen thickness	Average maximum displacement	Average maximum force P_c^{exp}
[mm]	[mm]	[mm]	[kN]
0.5	4.92	0.24	2.74
0.5	14.38	0.28	8.88
2	4.92	0.45	4.55
2	14.91	0.45	12.94
10	4.91	1.19	7.88
10	14.64	1.2	23.05

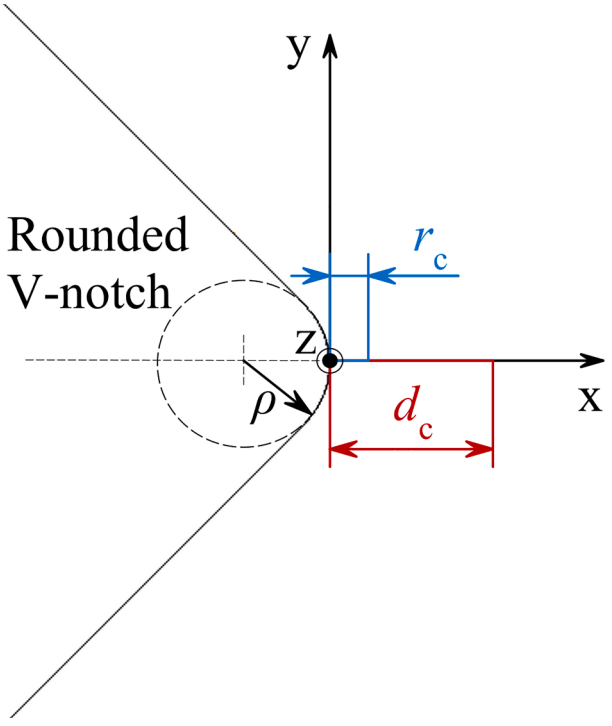

Fig. 3. The critical distances.

The fictitious material concept has also been applied to ductile materials, but in cases where large deformations are observed at failure. This concept also assumes that the SED for the real ductile material and the brittle virtual material are the same. In this case, the strain values of the real and virtual materials corresponding to the tensile strength (ultimate point) of the real material are assumed to be equal. This forces the determination of the Young's modulus value of the virtual material. In order to use this concept in conjunction with the MTS and MS criteria, the values of the following parameters were determined. The Young's modulus value for virtual material E^{FMC} was calculated based on (see Fig. 5):

$$\boldsymbol{SED} = \int_0^{\varepsilon_u} E^{FMC}\varepsilon d\varepsilon \rightarrow E^{FMC} = \frac{2(\boldsymbol{SED})}{\varepsilon_u^2} \tag{3.6}$$

Next, the tensile strength of the virtual material σ_f^{FMC} was determined as before but taking into account the value of the Young's modulus of virtual material E^{FMC}:

$$\boldsymbol{SED} = \frac{\left(\sigma_f^{FMC}\right)^2}{2E^{FMC}} \rightarrow \sigma_f^{FMC} = \sqrt{2E^{FMC}\boldsymbol{SED}} \tag{3.7}$$

The values of critical distances were determined based on Eqs. (3.3)-(3.4), where $\sigma_c = \sigma_f^{FMC}$ and K_{IC} is taken from Table 1.

The approaches used above are based on a comparison of strain energy for real and virtual materials. Similar assumptions are used, for example, to calculate local elastic–plastic stresses and strains in the notch bottom. In the work of Molski and Glinka [42], the theoretical stress concentration factor was related to the unit elastic strain energy in the notch. It was shown that the relationship described in the paper enables accurate results to be obtained even if the material shows pronounced plasticisation. Greater accuracy of the method relative to the use of Neuber's rule [43] was indicated.

4. Finite element analysis

Using the previously discussed fracture criteria to predict the fracture phenomenon in structural elements requires knowledge of the stress distributions around the notch bottom. For this purpose, linear numerical calculations were carried out using the finite element method (FEM) conducted in the MSC Marc Mentat environment. Models of notched specimens were described by QUAD8-type finite elements; the size of the finite element describing the region of interest, i.e. the notch bottom, was selected by determining the convergence of the solution. Due to the use of 2D elements, the model was not simplified using symmetry conditions, the entire specimen was modelled and its thickness was described parametrically. The boundary conditions were set as in Fig. 6. A linear-elastic material model was adopted. The convergence of the numerical model was established by decreasing the size of the finite element (increasing the total number of elements in the numerical model) near the notch bottom, until a subsequent change in element size did not cause significant changes in the value of the maximum principal stress. The Fig. 7 shows, using the example of a notched specimen with a bottom rounding radius of 10 mm (linear elastic material, maximum load determined experimentally), how the stress value changes as a function of the finite element size (Fig. 7a) and the number of finite elements of the model numerical (Fig. 7b).

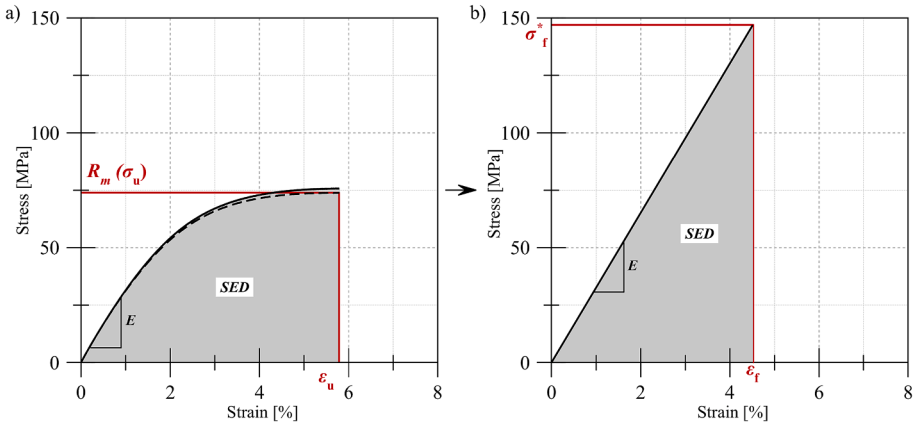

Fig. 4. A) the stress–strain curve for real nonlinear material (PMMA) and b) the stress–strain curve for equivalent brittle material (EMC).

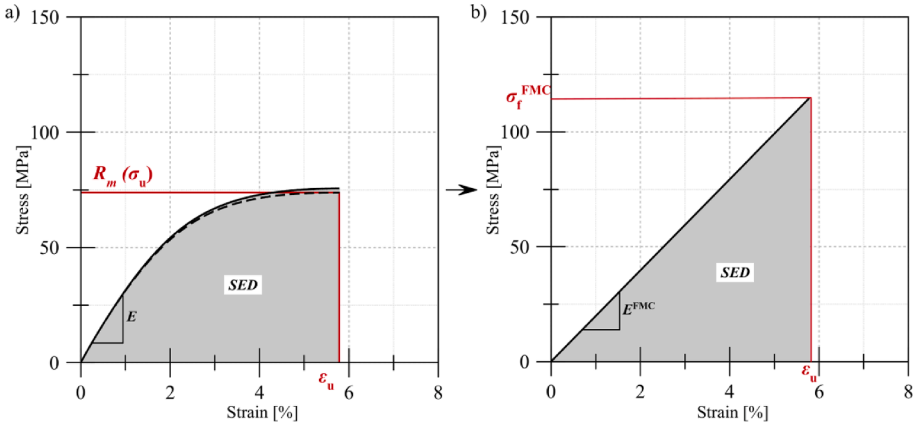

Fig. 5. A) the stress–strain curve for real nonlinear material (PMMA) and b) the stress–strain curve for fictitious brittle material (FMC).

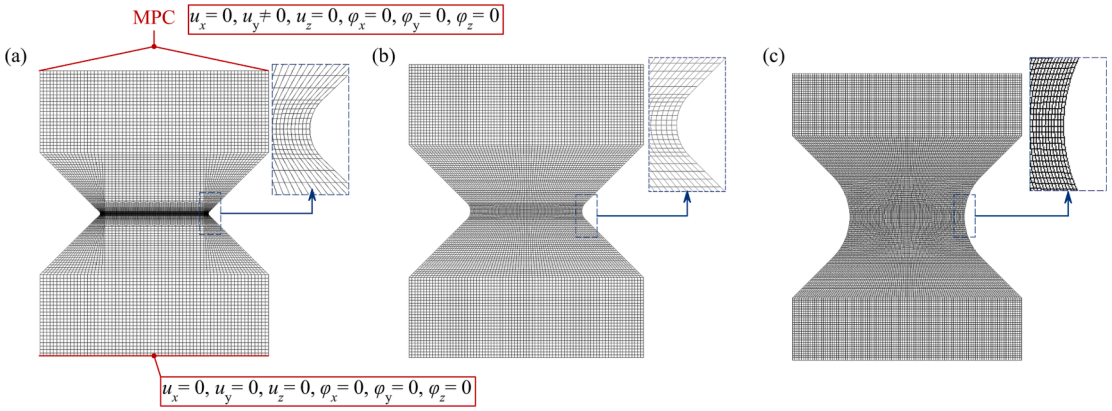

Fig. 6. The finite element mesh and boundary conditions for notched specimens with bottom rounding radius equal to: a) 0.5 mm, b) 2 mm, and c) 10 mm.

The purpose of the calculations was to determine the value of the critical load, i.e. the value of the tensile force at which, according to a given criterion, crack initiation occurred. In the calculations, a tensile force of $P_0 = 1000$ N was set, at which the values of tangential stress and average normal stress were determined based on the previously determined values of critical distances. Using the proportional increase of the stress value with respect to the value of the applied force, the critical load values were calculated according to the relation:

$$P_c = \frac{\sigma_c}{\sigma_{\theta\theta}} \cdot P_0 \tag{4.1}$$

or

$$P_c = \frac{\sigma_c}{\sigma_n} \cdot P_0 \tag{4.2}$$

Depending on the criterion being verified, the critical stress values σ_c varied. The parameters used for the criteria are summarised in Table 3. I should be underlined that to compute the critical distances, the stresses after the ultimate point were not used. To compute the critical distances for MS and MTS fracture criteria, the ultimate tensile strength of the real PMMA was used. In the case of EMC and FMC, the tensile strength of the

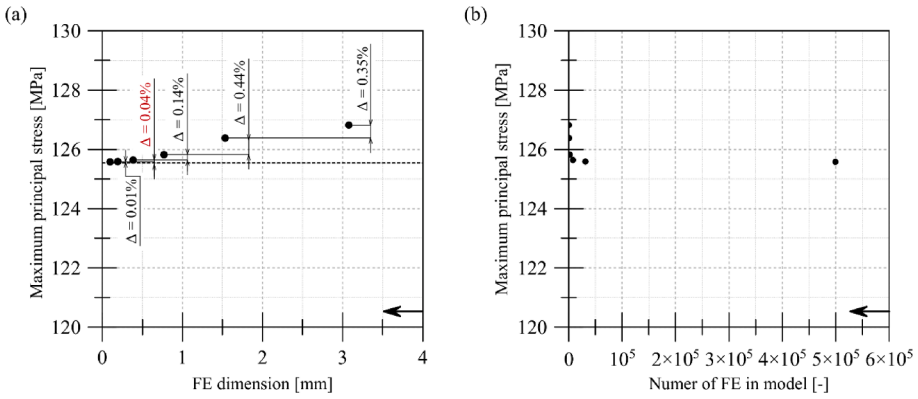

Fig. 7. Convergence of the solution based on the results obtained for specimens with bottom rounding radius equal to 10 mm: (a) the value of the maximum principal stress as a function of the finite element dimension and (b) the value of the maximum principal stress as a function of the total number of elements in numerical model.

Table 3
Values of the parameters used in the verified fracture criteria.

Criterion	Young's modulus [MPa]	Critical distances [mm]	Critical stress σ_c [MPa]
MTS	$E = 3\,254$	$r_c = 0.035$	$\sigma_u = 72.10$
MS		$d_c = 0.140$	
MTS + EMC		$r_c = 0.008$	$\sigma_f^* = 146.92$
MS + EMC		$d_c = 0.034$	
MTS + FMC	$E^{FMC} = 1\,984$	$r_c = 0.014$	$\sigma_f^{FMC} = 114.72$
MS + FMC		$d_c = 0.055$	

Equivalent Material and Fictitious Material are respectively used for this purpose, which are not directly related to the real PMMA, but related to the two virtual linear elastic materials.

5. Experimental calibration – Critical parameters calculations with TCD

The values of critical distances and critical stress used in the criteria discussed above were determined alternatively based on the classical theory of critical distances (TCD) formulas [44]. An attempt was made to determine the values of these parameters from the experimental data.

Linear elastic FE analyses of the test specimens with critical loading conditions were carried out on the basis of the experimentally obtained data. The finite element mesh and boundary conditions discussed earlier were used. Fig. 8 shows the relationship between the maximum principal stress and the distance from the notch bottom. The experimental value of r_c and σ_t was read from the point on the graph (see Fig. 8).

Fig. 8 shows how the critical parameter values were determined separately for specimens of different thicknesses. It is noted that the thickness of the element affects the values of stress and critical distance r_c. For specimens with a nominal thickness of $t = 5$ mm, the parameter values were determined as the geometric centre of all intersection points. On this basis, $r_c = 0.072$ mm and $\sigma_t = 128.55$ MPa were determined (Fig. 8a). In the case of elements of thickness $t = 15$ mm, all the obtained curves converged at a single point of intersection which its coordinates indicated: $r_c = 0.097$ mm and $\sigma_t = 122.92$ MPa (Fig. 8b). It should be noted that in the case of the PMMA tested, and probably other thermoplastics, the critical parameters will also depend on the thickness of the sample. The values obtained on the basis of the experimental calibration differ from those determined on the basis of classical TCD relationships (Table 3), especially the values of parameter r_c are different. Analysing the stress curve as a function of distance from the notch bottom for thin specimens, it can be seen that after discarding a specimen with a notch root radius of $\rho = 10$ mm (for which the relationship is similar to that of unnotched specimens), the parameter r_c reaches a value close to that determined from equation (3.2). The same parameter determined for thick specimens reaches a value twice as large. In the cases that critical stresses are responsible for crack initiation, experimental calibration yielded the value closest to the stresses determined using FMC.

The critical parameters determined from experimental calibration (Fig. 8) were used to predict fracture initiation and the results are summarised in the next section of the paper.

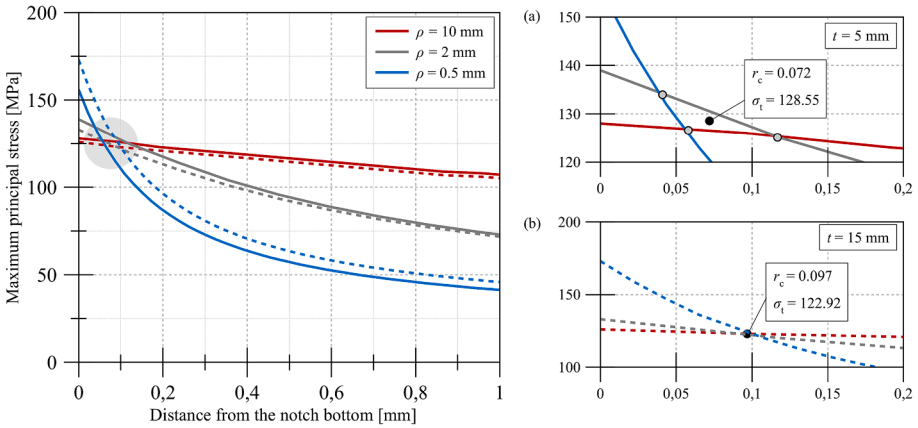

Fig. 8. Critical distance and critical stress values obtained from TCD using experimental calibration: (a) $t = 5$ mm and (b) $t = 15$ mm.

6. Results and discussion

The results of numerical calculations in the form of the critical tensile force value determined from the stress distributions in the notch bottom. The formulas (3.8) – (3.9) and the data included in Table 3 were compared with the results of the experimental tests (Table 2). The results are summarised in Table 4 and Figs. 9 and 10. The relative deviation between the experimental and theoretical critical load values was indicated as:

$$\Delta = \frac{P_c^{exp} - P_c}{P_c^{exp}}[\%] \tag{6.1}$$

Prediction of the critical load value in notched PMMA specimens using classical fracture criteria such as MS and MTS is subject to high error. The obtained force values, regardless of the radius of the rounded bottom of the notch, are on average 41 % and 45 % lower than the experimental value for the MS and MTS criteria, respectively (Figs. 9 and 10, green). These discrepancies are mainly due to the low value of the critical stresses assumed in the above formulas. These elements carry much higher stresses than those determined by the tensile strength determined for the smooth specimen.

These criteria perform much better when combined with the EMC. The MS + EMC and MTS + EMC criteria, applied to specimens with a notch root radius of $\rho = 0.5$ mm, yielded a critical tensile force value close to the experimental value; errors of about 3 % for the thin specimen and about 9 % for the thick specimen were obtained, with the MS + EMC criterion performing much better. Improvements in the result in predicting the critical load value, compared to the classical MS and MTS criteria, were also noted for the remaining radii of $\rho = 2$ mm (7 %, 10 %) and 10 mm (15 %, 17 %) for thin and thick specimens, respectively. The discrepancies for both MS + EMC and MTS + EMC criteria are at the same level. It should be noted, however, that for radii $\rho = 2$ mm and 10 mm, the use of EMC allowed greater convergence to be obtained with the experimental data, but the values obtained are higher than the actual critical load values (Figs. 9 and 10 – red). Thus, the use of MS + EMC and MTS + EMC to predict fracture in notch-weakened PMMA components with radii greater than 0.5 mm may lead to overestimation of the critical load value, and thus lead to crack initiation during the service life of the member.

A further development of the MS and MTS criteria was the use of the FMC. This approach definitely works well in predicting fracture in notched specimens with larger bottom rounding radii (Figs. 8 and 9 – blue). For $\rho = 10$ mm, deviations of 10 % and 8 % were held for thin and thick specimens, respectively, regardless of the MS + FMC and MTS + FMC criteria used. This produces results much closer to the experimental ones than using EMC, and the calculated load value is lower than the actual one. This provides confidence in the safe working conditions of the component. In the case of a notch with a radius of $\rho = 2$ mm, the FMC concept used together with the MS and MTS criteria yielded results different from the experimental value by about 16 % and 14 % for thin and thick specimens, respectively. The deviation is larger than when using EMC, but again it should be noted that values lower than the experimental value were obtained, so if the work of the component is limited by this load value, one can be sure that crack initiation will not occur. The least favourable results in this comparison were for $\rho = 0.5$ mm.

The MTS and MS criteria were also used to implement the values of critical parameters determined by experimental calibration (denoted as MTS + exp and MS + exp in Table 4).

Very good results were obtained using the MTS criterion. This method proved to be the most effective of all those presented (Figs. 9 and 10 – orange). An average relative error of 3 % was obtained, with the largest discrepancy between the experimental and criterion-determined critical load value, and was 8 % for specimens with a thickness of 5 mm weakened with a notch with a radius $\rho = 0.5$ mm. The proposed method does not work for the MTS criterion, as averaging the stress values over quite a large critical distance causes significant errors. In conclusion, the use of parameters determined by experimental calibration allows the values of critical load to be determined with high accuracy using the criterion of tangential stress. It should be emphasised that this approach requires tensile tests for specimens with different notch root radii. In this case, the thickness of these elements is also important – this parameter affects the stress values observed near the notch bottom. Conducting such extensive tests is not always possible.

The elements discussed in the present paper were also used to carry out nonlinear numerical calculations, in which PMMA was described using an elastoplastic material model. The linear elastic part of the work was described using the Young's modulus and Poisson's ratio, while the plastic part was described using a hardening curve determined from the actual tensile stress–strain curve (Fig. 1). The specimens were loaded with the critical force value obtained from the experimental tests. Fig. 11 shows the equivalent stress distributions for all tested specimens, including the yield zone - stresses higher than those corresponding to $R_{0.2} = 47.17$ MPa [31] are marked. Depending on the notch root radius, different sizes of the yield zone are observed. The larger the radius ρ, the larger the size of the zone where permanent deformation occurred. Measurements were made of the size of this area along the symmetry axis of the notches and the largest dimension along the loading direction. For notched elements with the largest bottom rounding radius $\rho =$ 10 mm, permanent deformation was observed practically throughout the entire area of the specimen. Plastic deformation extended along the notch axis of symmetry for an average distance of about 0.72 mm for a radius of $\rho = 0.5$ mm and 2.32 mm for $\rho = 2$ mm. Similar results of measuring the size of the yield zone are presented in the work of Torabi et al. [23] on the example of U-type notches.

In the case of $\rho = 0.5$ mm, the yielding zone is very small (it can be classified as so-called small scale yielding), so for the most part the

Table 4
Results of numerical calculations and the relative deviation between the theoretical and experimental critical load values.

Notch root radius [mm]	Nominal thickness [mm]	Critical force P_c [kN]			
		MTS	**Δ [%]**	**MS**	**Δ [%]**
0.5	5	1.57	**43**	1.87	**32**
0.5	15	4.60	**48**	5.47	**38**
2	5	2.44	**46**	2.51	**45**
2	15	7.12	**45**	7.34	**43**
10	5	4.48	**43**	4.50	**43**
10	15	13.32	**42**	13.42	**42**
		MTS + EMC	**Δ [%]**	**MS + EMC**	**Δ [%]**
0.5	5	2.66	**3**	2.83	**−3**
0.5	15	7.78	**12**	8.26	**7**
2	5	4.85	**−7**	4.88	**−7**
2	15	14.17	**−10**	14.27	**−10**
10	5	9.05	**−15**	9.07	**−15**
10	15	26.99	**−17**	27.04	**−17**
		MTS + FMC	**Δ [%]**	**MS + FMC**	**Δ [%]**
0.5	5	2.13	**22**	2.40	**12**
0.5	15	6.22	**30**	7.01	**21**
2	5	3.81	**16**	3.85	**15**
2	15	11.12	**14**	11.26	**13**
10	5	7.08	**10**	7.10	**10**
10	15	21.11	**8**	21.17	**8**
		MTS + exp	**Δ [%]**	**MS + exp**	**Δ [%]**
0.5	5	2.97	**−8**	4.05	**−48**
0.5	15	8.89	**0**	11.58	**−30**
2	5	4.49	**1**	4.77	**3**
2	15	12.54	**5**	13.41	**−4**
10	5	8.03	**−2**	8.15	**0**
10	15	2.99	**−3**	23.47	**−2**

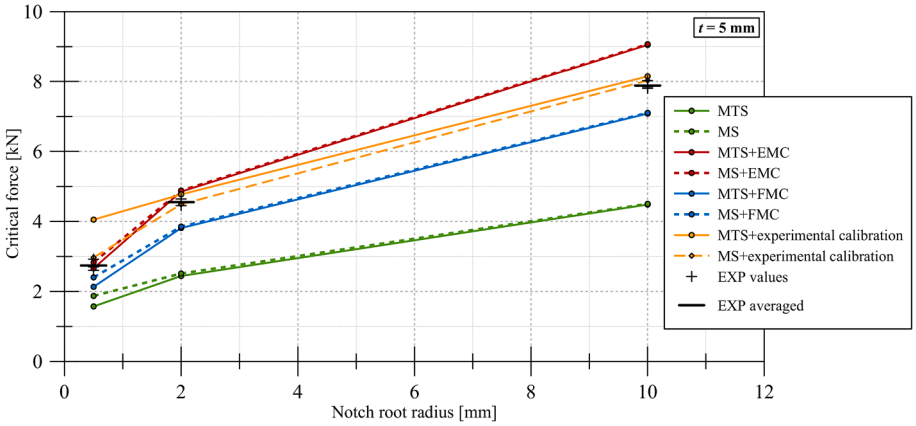

Fig. 9. The theoretical and experimental critical load values for different root radii and specimen nominal thickness $t = 5$ mm.

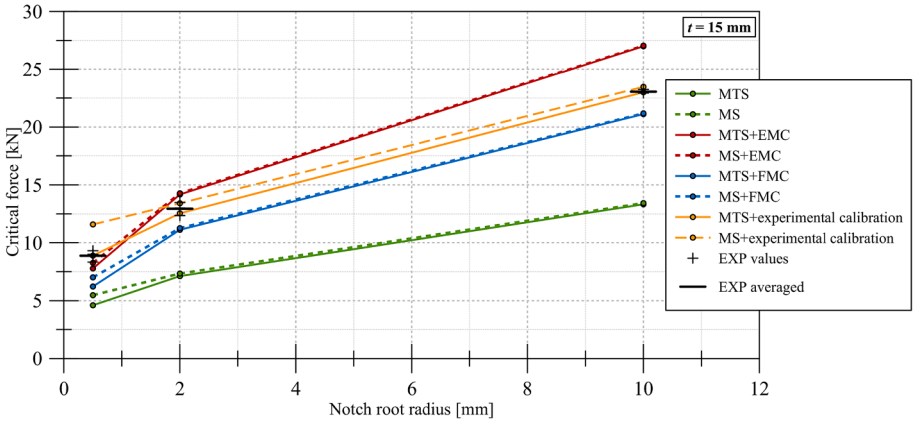

Fig. 10. The theoretical and experimental critical load values for different root radii and specimen nominal thickness $t = 15$ mm.

material works in a linear elastic range, hence the rather high effectiveness of using EMC criteria to predict critical load. The larger the radius of rounding the larger the area of plasticisation; in the case of radii ρ = 2 mm and ρ = 10 mm large scale yielding can be considered. In these cases, by far the more effective concept is FMC. It should be emphasised that both approaches to fracture prediction, EMC and FMC, are effective, but their use should be strictly dependent on the radius of the bottom of the notch, and thus the level of plastic deformation. The specimens with ρ = 10 mm notch tip radius experience Gross Yielding (GY), which means that the entire ligament is saturated by plastic deformation.

For specimens with a notch tip radius of 10 mm, where the entire ligament is saturated with plastic deformation, the value of the critical load can be easily estimated using the formula for normal stress in tension:

$$\sigma_u = \frac{P_c}{A_0} \tag{6.2}$$

where: σ_u – tensile strength [MPa], P_c – critical force and A_0 – nominal cross-sectional cross area [mm^2]. Using this relationship, critical force values were determined. Critical load values were obtained equal to 7.08 kN for thin and 23.05 kN for thick specimens. As can be seen, these values differ from the experimental ones by only 10 % and 8 %, respectively. For specimens with notches with a radius $\rho = 2$ mm and $\rho = 0.5$ mm, the large stress gradients near the notch bottom do not allow the critical load value to be determined using the relationship described above. The discrepancies between the experimental and theoretical values of the critical force reach 50 and even 150 %, corresponding to $\rho = 2$ mm and $\rho = 0.5$ mm.

7. Conclusions

The purpose of this study was to evaluate the effectiveness of fracture criteria available in the literature used to estimate the critical load value, i.e. the critical tensile force value during fracture of flat notched PMMA specimens. The conclusions of the work are presented below.

Classical brittle fracture criteria do not always work well for predicting critical load values for plastic materials such as PMMA, particularly large errors occur when the material is tested under conditions where it exhibits considerable plastic strains under tension.

The EMC and FMC provide a more accurate indication of the critical load in test specimens, but their effectiveness depends on the notch root radius, and thus the size of the plastic zone.

The EMC in combination with MS and MTS criteria work better for the small notch root radii($\rho = 0.5$ mm)– a small yield zone.

The FMC in combination with MS and MTS criteria perform better for large notch root radii ($\rho = 2$ mm and $\rho = 10$ mm) – large yield zones.

The work may continue with the use of HEX finite elements in FEM modelling, likely contributing to better results for thicker specimens in particular.

CRediT authorship contribution statement

Elżbieta Bura: Writing – original draft, Visualization, Resources, Methodology, Investigation, Funding acquisition, Formal analysis, Data curation, Conceptualization. **A.R. Torabi:** Writing – review & editing,

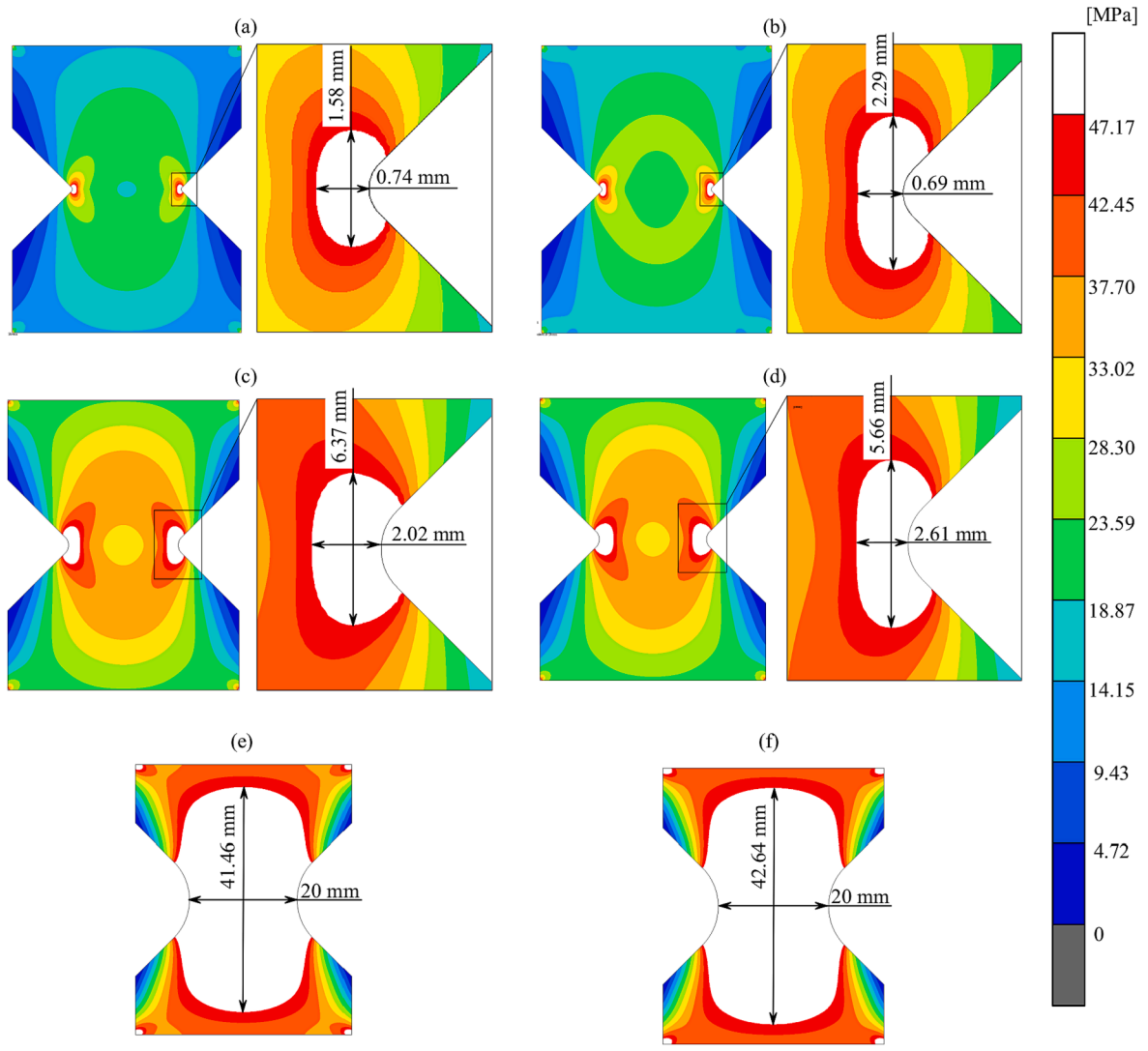

Fig. 11. Equivalent stress distributions around notches in the PMMA specimens under critical loads: (a), (b) notch tip radius of 0.5 mm, (c), (d) 2 mm, and (e), (f) 4 mm. Specimens nominal thickness (a), (c), and (e) equal to 5 mm and (b), (d), and (f) equal to 15 mm.

Supervision, Methodology, Formal analysis, Conceptualization. **Andrzej Seweryn:** Writing – review & editing, Supervision, Investigation.

Declaration of competing interest

The authors declare that they have no known competing financial interests or personal relationships that could have appeared to influence the work reported in this paper.

Data availability

Data will be made available on request.

Acknowledgements

This research was funded by the National Science Centre Poland based on project no 2019/33/N/ST8/02382.

The datasets used and/or analysed during the current study available from the corresponding author on reasonable request.

References

[1] A. Seweryn, Brittle fracture criterion for structures with sharp notches, Eng. Fract. Mech. 47 (5) (1994) 673–681, https://doi.org/10.1016/0013-7944(94)90158-9.

[2] V.V. Novozhilov, On a necessary and sufficient criterion for brittle strength, J. Appl. Math. Mech. 33 (2) (Jan. 1969) 201–210, https://doi.org/10.1016/0021-8928(69)90025-2.

[3] M. R. Ayatollahi, M. Rashidi Moghaddam, S. M. J. Razavi, and F. Berto, 'Geometry effects on fracture trajectory of PMMA samples under pure mode-I loading', *Eng Fract Mech*, vol. 163, pp. 449–461, Sep. 2016, 10.1016/j.engfracmech.2016.05.014.

[4] G.C. Sih, Strain-energy-density factor applied to mixed mode crack problems, Int J Fract 10 (3) (Sep. 1974) 305–321, https://doi.org/10.1007/BF00035493.

[5] M.R.M. Aliha, S.S. Samareh-Mousavi, M.M. Mirsayar, Loading rate effect on mixed mode I/II brittle fracture behavior of PMMA using inclined cracked SBB specimen, Int J Solids Struct 232 (Dec. 2021) 111177, https://doi.org/10.1016/j.ijsolstr.2021.111177.

[6] E. Bura and A. Seweryn, 'Fracture initiation in notched specimens subjected to compression: Strain rate effect', *Materials*, vol. 13, no. 11, 2020, 10.3390/ma13112613.

[7] S. Acharya, A.K. Mukhopadhyay, High strain rate compressive behavior of PMMA, Polym. Bull. 71 (1) (Jan. 2014) 133–149, https://doi.org/10.1007/s00289-013-1050-9.

[8] H. Wada, M. Seika, T.C. Kennedy, C.A. Calder, K. Murase, Investigation of loading rate and plate thickness effects on dynamic fracture toughness of PMMA, Eng. Fract. Mech. 54 (6) (Jul. 1996) 805–811, https://doi.org/10.1016/0013-7944(95)00244-8.

[9] P. Foti, N. Razavi, F. Berto, Fracture assessment of U-notched PMMA under mixed mode I/II loading conditions by means of local approaches, Procedia Struct. Integrity 33 (2021) 482–490, https://doi.org/10.1016/j.prostr.2021.10.055.

[10] P. Lazzarin, R. Zambardi, A finite-volume-energy based approach to predict the static and fatigue behavior of components with sharp V-shaped notches, Int. J. Fract. 112 (3) (2001) 275–298, https://doi.org/10.1023/A:1013595930617.

[11] J. Zhong, J. Wang, X. Li, X. Chu, Experiments and discrete element simulations of crack initiation angle of mixed-mode I/II in PMMA material, Theor. Appl. Fract. Mech. 125 (Jun. 2023) 103862, https://doi.org/10.1016/j.tafmec.2023.103862.
[12] F.J. Gómez, M. Elices, Fracture of components with V-shaped notches, Eng. Fract. Mech. 70 (14) (Sep. 2003) 1913–1927, https://doi.org/10.1016/S0013-7944(03)00131-0.
[13] E. Bura, A. Seweryn, Mode I fracture in PMMA specimens with notches – Experimental and numerical studies, Theor. Appl. Fract. Mech. 97 (Oct. 2018) 140–155, https://doi.org/10.1016/j.tafmec.2018.08.002.
[14] M.R. Ayatollahi, A.R. Torabi, B. Bahrami, On the necessity of using critical distance model in mixed mode brittle fracture prediction of V-notched Brazilian disk specimens under negative mode I conditions, Theor. Appl. Fract. Mech. 84 (Aug. 2016) 38–48, https://doi.org/10.1016/j.tafmec.2016.01.001.
[15] A.R. Torabi, B. Bahrami, M.R. Ayatollahi, Mixed mode I/II brittle fracture in V-notched Brazilian disk specimens under negative mode I conditions, Phys. Mesomech. 19 (3) (Jul. 2016) 332–348, https://doi.org/10.1134/S1029959916030115.
[16] B. Bahrami, M.R. Ayatollahi, A. Torabi, Predictions of fracture load, crack initiation angle, and trajectory for V-notched Brazilian disk specimens under mixed mode I/II loading with negative mode I contributions, Int. J. Damage Mech 27 (8) (Aug. 2018) 1173–1191, https://doi.org/10.1177/1056789517726360.
[17] M.R. Ayatollahi, M.R.M. Aliha, M.M. Hassani, Mixed mode brittle fracture in PMMA—An experimental study using SCB specimens, Mater. Sci. Eng. A 417 (1–2) (Feb. 2006) 348–356, https://doi.org/10.1016/j.msea.2005.11.002.
[18] M. Ataei-Aazam, M. Safarabadi, M. Beygzade, N.M. Khansari, Numerical & experimental assessment of mixed-modes (I/II) fracture of PMMA/hydroxyapatite nanocomposite, Theor. Appl. Fract. Mech. 123 (Feb. 2023) 103737, https://doi.org/10.1016/j.tafmec.2022.103737.
[19] M. Safarabadi, N. Mehri Khansari, A. Rezaei, An experimental investigation of HA/AL2O3 nanoparticles on mechanical properties of restoration materials, Eng. Solid Mech. 2 (3) (2014) 173–182, https://doi.org/10.5267/j.esm.2014.4.006.
[20] A.R. Torabi, Estimation of tensile load-bearing capacity of ductile metallic materials weakened by a V-notch: The equivalent material concept, Mater. Sci. Eng. A 536 (Feb. 2012) 249–255, https://doi.org/10.1016/j.msea.2012.01.007.
[21] A.R. Torabi, M. Alaei, Mixed-mode ductile failure analysis of V-notched Al 7075–T6 thin sheets, Eng. Fract. Mech. 150 (Dec. 2015) 70–95, https://doi.org/10.1016/j.engfracmech.2015.10.037.
[22] A.R. Torabi, E. Pirhadi, Stress-based criteria for brittle fracture in key-hole notches under mixed mode loading, Eur. J. Mech. A. Solids 49 (Jan. 2015) 1–12, https://doi.org/10.1016/j.euromechsol.2014.06.009.
[23] A.R. Torabi, S. Shahbaz, S. Cicero, M.R. Ayatollahi, Fracture testing and estimation of critical loads in a PMMA-based dental material with nonlinear behavior in the presence of notches, Theor. Appl. Fract. Mech. 118 (Apr. 2022) 103282, https://doi.org/10.1016/j.tafmec.2022.103282.
[24] S. Cicero, A.R. Torabi, V. Madrazo, P. Azizi, Prediction of fracture loads in PMMA U-notched specimens using the equivalent material concept and the theory of critical distances combined criterion, Fatigue Fract. Eng. Mater. Struct. 41 (3) (Mar. 2018) 688–699, https://doi.org/10.1111/ffe.12728.
[25] A.R. Torabi, M. Kamyab, The fictitious material concept, Eng. Fract. Mech. 209 (Mar. 2019) 17–31, https://doi.org/10.1016/j.engfracmech.2019.01.022.
[26] A.R. Torabi, M. Kamyab, Mixed mode I/II failure prediction of thin U-notched ductile steel plates with significant strain-hardening and large strain-to-failure: The Fictitious Material Concept, Eur. J. Mech. A. Solids 75 (May 2019) 225–236, https://doi.org/10.1016/j.euromechsol.2019.02.004.
[27] A.R. Torabi, B. Saboori, A. Ghelich, Fracture of U- and V-notched Al6061-T6 plates: The first examination of the Fictitious Material Concept under mixed mode I/III loading, Theor. Appl. Fract. Mech. 109 (Oct. 2020) 102766, https://doi.org/10.1016/j.tafmec.2020.102766.
[28] A.R. Torabi, H. Sadeghian, M.R. Ayatollahi, Mixed mode I/II crack propagation in stainless steel 316L sheets by large plastic deformations: Prediction of critical load by combining LEFM with fictitious material concept, Eng. Fract. Mech. 247 (Apr. 2021) 107657, https://doi.org/10.1016/j.engfracmech.2021.107657.
[29] A.R. Torabi, H. Talebi, M.R. Ayatollahi, M. Petru, Mixed mode I-III fracture resistance of stainless steel 316L weakened by V-notches with end holes, Theor. Appl. Fract. Mech. 122 (Dec. 2022) 103574, https://doi.org/10.1016/j.tafmec.2022.103574.
[30] S. Cicero, A.R. Torabi, H.R. Majidi, F.J. Gómez, On the use of the combined FMC-ASED criterion for fracture prediction of notched specimens with nonlinear behavior, Procedia Struct. Integrity 28 (2020) 84–92, https://doi.org/10.1016/j.prostr.2020.10.011.
[31] E. Bura, A. Seweryn, The fracture behaviour of notched PMMA specimens under simple loading conditions – Tension and torsion experimental tests, Eng. Fail. Anal. 148 (Jun. 2023) 107199, https://doi.org/10.1016/j.engfailanal.2023.107199.
[32] Y. Du, P. Pei, T. Suo, G. Gao, Large deformation mechanical behavior and constitutive modeling of oriented PMMA, Int. J. Mech. Sci. 257 (Nov. 2023) 108520, https://doi.org/10.1016/j.ijmecsci.2023.108520.
[33] Y. Yan, Y. Sun, J. Su, B. Li, P. Zhou, Crazing Initiation and Growth in Polymethyl Methacrylate under Effects of Alcohol and Stress, Polymers (basel) 15 (6) (Mar. 2023) 1375, https://doi.org/10.3390/polym15061375.
[34] B. Zheng, S. Zhang, G. Shu, Z. Sun, Y. Wang, J. Xie, Experimental investigation and modeling of the mechanical properties of construction PMMA at different temperatures, Structures 57 (Nov. 2023) 105091, https://doi.org/10.1016/j.istruc.2023.105091.
[35] P. Qiu, Z. Yue, R. Yang, Mode I stress intensity factors measurements in PMMA by caustics method: A comparison between low and high loading rate conditions, Polym Test 76 (Jul. 2019) 273–285, https://doi.org/10.1016/j.polymertesting.2019.03.029.
[36] A. Wiangkham, A. Ariyarit, P. Aengchuan, Prediction of the mixed mode I/II fracture toughness of PMMA by an artificial intelligence approach, Theor. Appl. Fract. Mech. 112 (Apr. 2021) 102910, https://doi.org/10.1016/j.tafmec.2021.102910.
[37] F. Erdogan, G.C. Sih, On the Crack Extension in Plates Under Plane Loading and Transverse Shear, J. Basic Eng. 85 (4) (Dec. 1963) 519–525, https://doi.org/10.1115/1.3656897.
[38] S. Safaei, M.R. Ayatollahi, B. Saboori, Fracture behavior of GPPS brittle polymer under mixed mode I/III loading, Theor. Appl. Fract. Mech. 91 (Oct. 2017) 103–115, https://doi.org/10.1016/j.tafmec.2017.04.017.
[39] R.O. Ritchie, J.F. Knott, J.R. Rice, On the relationship between critical tensile stress and fracture toughness in mild steel, J. Mech. Phys. Solids 21 (6) (Nov. 1973) 395–410, https://doi.org/10.1016/0022-5096(73)90008-2.
[40] F.J. Gómez, G.V. Guinea, M. Elices, Failure criteria for linear elastic materials with U-notches, Int. J. Fract. 141 (1–2) (Sep. 2006) 99–113, https://doi.org/10.1007/s10704-006-0066-7.
[41] L. Susmel, D. Taylor, The theory of critical distances to predict static strength of notched brittle components subjected to mixed-mode loading, Eng. Fract. Mech. 75 (3–4) (Feb. 2008) 534–550, https://doi.org/10.1016/j.engfracmech.2007.03.035.
[42] K. Molski, G. Glinka, A method of elastic-plastic stress and strain calculation at a notch root, Mater. Sci. Eng. 50 (1) (Sep. 1981) 93–100, https://doi.org/10.1016/0025-5416(81)90089-6.
[43] H. Neuber, Theory of Stress Concentration for Shear-Strained Prismatical Bodies With Arbitrary Nonlinear Stress-Strain Law, J. Appl. Mech. 28 (4) (Dec. 1961) 544–550, https://doi.org/10.1115/1.3641780.
[44] The Theory of Critical Distances. Elsevier, 2007. 10.1016/B978-0-08-044478-9.X5000-5.